Bioorganic & Medicinal Chemistry Letters 20 (2010) 326–329

Contents lists available at ScienceDirect

Bioorganic & Medicinal Chemistry Letters

journal homepage: www.elsevier.com/locate/bmcl

Pyrazolone based TGFβR1 kinase inhibitors

Kevin Guckian *, Mary Beth Carter, Edward Yin-Shiang Lin, Michael Choi, Lihong Sun, P. Ann Boriack-Sjodin, Claudio Chuaqui, Benjamin Lane, Kam Cheung, Leona Ling, Wen-Cherng Lee

Biogen Idec Inc., 14 Cambridge Center, Cambridge, MA 02142, USA

ARTICLE INFO

Article history:
Received 26 August 2009
Revised 21 October 2009
Accepted 26 October 2009
Available online 29 October 2009

Keywords:
TGFβ
Pyrazolone
Kinase inhibitors

ABSTRACT

Interruption of TGFβ signaling through inhibition of the TGFβR1 kinase domain may prove to have beneficial effect in both fibrotic and oncological diseases. Herein we describe the SAR of a novel series of TGFβR1 kinase inhibitors containing a pyrazolone core. Most TGFβR1 kinase inhibitors described to date contain a core five-membered ring bearing N as H-bond acceptor. Described herein is a novel strategy to replace the core structure with pyrazolone ring, in which the carbonyl group is designed as an H-bond acceptor to interact with catalytic Lys 232.

TGFβ signaling is involved in a wide variety of physiological processes. Inhibition of TGFβ signaling has been shown to provide therapeutic benefit in preclinical models in fibrosis and oncology.[1,2] Currently, several antibodies and antisense oligonucleotides that interrupt TGFβ signaling are progressing through clinical trials for treatment in both fibrotic disease and oncology. Inhibition of the kinase domain of TGFβR1 which is responsible for propagation of the downstream signal after TGFβ binding to the receptor represents another strategy for TGFβ pathway inhibition. We therefore sought to design selective ATP competitive inhibitors of TGFβ signaling by inhibition of the TGFβR1 kinase domain.

We and others have previously described vicinal bisaryl heterocycles as potent and selective inhibitors of TGFβR1 (Fig. 1).[1,3–6] In an effort to expand diversity and improve the in vivo properties of this class of inhibitors the nature of the heterocycle core was investigated. Through modeling studies the pyrazolone heterocycle was identified as a promising five-membered heterocyclic core. The carbonyl group of pyrazolone was designed to capture the HB interaction with Lys 232. Herein we describe the synthesis, SAR, structural characterization, and in vivo properties of this class of TGFβR1 kinase inhibitors.

The consensus binding mode for the vicinal bisaryl heterocycle class of inhibitors is well understood from co-crystal structures of both pyrazole[6] and imidazole (manuscript in preparation) based scaffolds. These studies show that one of the aromatic arms protrudes into the hydrophobic pocket formed due to the small serine gatekeeper found in TGFβR1 kinase. The other arm extends toward the hinge where at least one H-bonding contact is made. In addition, the core heterocycle itself makes a H-bonding interaction with Lys 232. Finally, in all members of this class of inhibitors described to date the moiety occupying the hydrophobic pocket needs to contain a basic nitrogen in the 2-position (2-pyridyl in most cases) to maintain good potency. Structural evidence suggests that the pyridyl nitrogen is part of a complex set of interactions between a bound water molecule, the protein, and the inhibitor. Through modeling it was predicted that the carbonyl of the pyrazolone core may obviate the need for the basic nitrogen in the 2-position, by interacting with both Lys 232 and the bound water molecule. Therefore, a series of 4-substituted pyrazolones were synthesized to test this hypothesis.

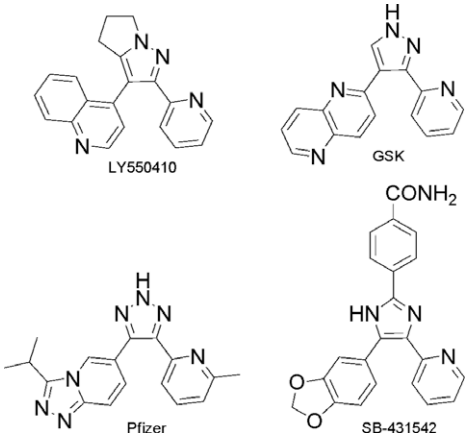

Figure 1. Structures of the literature described TGFβ inhibitors.

* Corresponding author.
E-mail address: kevin.guckian@biogenidec.com (K. Guckian).

0960-894X/$ - see front matter © 2009 Elsevier Ltd. All rights reserved.
doi:10.1016/j.bmcl.2009.10.108

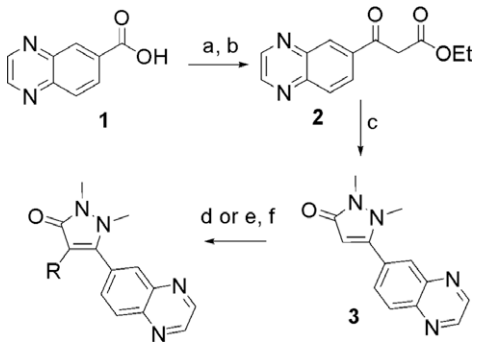

Scheme 1. Reagents and conditions: (a) EDC, DIPEA, *N,O*-dimethylhydroxylamine, DCM/DMF; (b) LDA, ethyl acetate, THF, −78 °C; (c) dimethylhydrazine, pyridine, 90° o/n; (d) $Pd(OAc)_2$, CsOAc, DMF, tri-(furyl)phosphine, aryl(heteroaryl)Br or aryl(heteroaryl)I 125°, o/n; (e) NBS, DCM, Δ; (f) $Pd(Dppf)_2$, dioxane, 2 M $NaCO_3$, aryl(heteroaryl boronic acid.

Synthesis of this class of inhibitors proceeded as shown in Scheme 1. Starting from the quinazoline acid **1** the Weinreb amide was formed. LDA deprotonation of ethyl acetate and displacement of the Weinreb amide gave ketoester **2**. Heating of ketoester **2** and dimethylhydrazine in pyridine gave pyrazolone **3** in good yield. Analog synthesis was accomplished by two separate routes. The first involves bromination of pyrazolone **3** with NBS and subsequent Suzuki coupling to give the final compound. The second more direct route was C–H activation of the pyrazolone with Pd in the presence of an Aryl bromide or iodide to give the final pyrazolone compounds.

A summary of TGFβR1 kinase inhibition activity by these analogs is reported in Tables 1–4. For reference SB-431542 (Fig. 1)

Table 1
Effect of pyridyl nitrogen on TGFpRl kinase inhibition

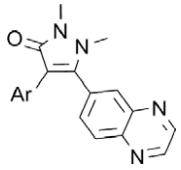

Compds	Ar	TGFβ K_i (μM)	TGFβ PAI-Luc IC_{50} (μM)
4	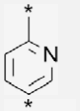	0.011	1.70
5	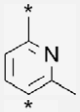	0.005	1.03
6	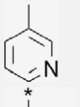	>2.80	nd
7	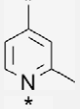	>2.80	nd
8	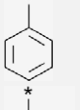	0.078	>10.0
9	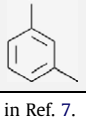	0.020	3.05

Assay description in Ref. 7.

Table 2
Effect of substitution position on TGFpRl Kinase inhibition

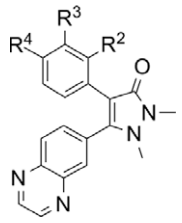

Compds	R^2	R^3	R^4	K_i (nM)	PAI-Luc IC_{50} (μM)
10	–OH	–H	–H	77	>10
11	–H	–OH	–H	53	>10
12	–H	–H	–OH	950	nd
13	$–NH_2$	–H	–H	952	nd
14	–H	$–NH_2$	–H	130	>10
15	–H	–H	$–NH_2$	640	nd
16	–CN	–H	–H	450	>10
17	–H	–CN	–H	45	>10

Assay description in Ref. 7.

Table 3
Effect of *meta* substitution on TGFβRI kinase activity

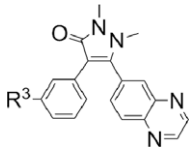

Compds	R^3	K_i (μM)	PAI-Luc IC_{50} (μM)
18	$–CH_2CH_3$	0.006	0.39
19	$–CHCH_2$	0.012	0.56
20	$–CH(CH_3)_2$	>2800	nd
21	$–SCH_3$	0.060	>10
22	–OCH3	0.020	1.4
23	$–CF_3$	0.111	1.1
24	$–CH_2OCH_3$	0.035	3.69
25	$–CH_2OH$	0.370	nd
26	$–CH_2NH_2$	>2800	nd
27	$–CH_2CN$	0.024	4.4
28	$–C(O)CH_3$	0.410	nd
29	$–C(O)NH_2$	>2800	nd
30	$–C(O)OCH_3$	0.440	nd
31	–F	0.078	0.99
32	–CI	0.019	1.9
33	–Br	0.012	0.22
34	$–NHSO_2Me$	0.019	>10
35	$–NHC(O)CH_3$	0.920	nd
36	$–NHSO_2CH_2CH_3$	>2800	nd
37	$–NHC(O)NHCH_3$	>2800	nd

Assay description in Ref. 7.

has a 17 nM K_i in the biochemical assay and a 250 nM IC_{50} in the PAI-Luc cellular assay. Table 1 shows the influence of basic nitrogens on TGFβRI kinase inhibition when placed in the hydrophobic pocket relative to their aromatic counterparts. The 2-pyridyl derivative compound **4** was found to be sevenfold more potent than phenyl and the 2-pyridyl-3-methyl derivative was found to be only fourfold more potent than *m*-tolyl. A similar trend was seen in a previously reported series with a pyrazole core.[8] Introduction of a basic nitrogen in the 3 or 4-position results in loss of inhibition.

These data prompted further exploration of simple aromatics. We first sought to define the optimal position for substitution on the aromatic ring. Table 2 shows that *meta* substitution of –OH, $–NH_2$, and –CN is superior to substitution in either the *ortho* or *para* position therefore the *meta* position was chosen for further exploration.

Table 4
Effect of heteroaromatics on TGFpRI kinase activity

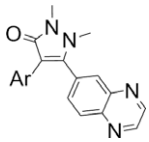

Compds	Ar	TGFβ K_i (μM)	TGFβ PAI-Luc IC_{50} (μM)
38		0.190	>10.0
39		0.073	>10.0
40		0.365	nd
41		0.054	>10.0
42	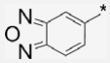	0.64	nd
43	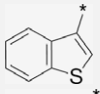	1.87	nd
44	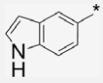	1.12	nd

Assay description in Ref. 7.

A large series of *meta* substituted inhibitors were synthesized (Table 3) in which the size, shape and polarity of the substituents were varied. Ethyl and ethylene substitution are the most potent compounds in the series and are approximately equipotent with the 2-pyridyl-3-methyl derivative described in Table 1. In general this position was very sensitive to the nature of substitution with preference for small hydrophobic substituents without branching on the alpha carbon.

Several heterocycles including bicycles were incorporated to further explore the hydrophobic pocket (Table 4). Small heterocycles were well tolerated with 3-substituted furan and thiophene approximately equipotent with phenyl. Surprisingly, 2-substitution of furan and thiophene results in a significant loss in potency. Finally, incorporation of bicycles leads to a large loss in potency regardless of substitution.

To confirm the binding hypothesis a co-crystal structure was obtained with compound **24** (PDB ID 3KCF). As predicted the carbonyl oxygen of the pyrazolone ring interacts with Lys 232 and the nitrogen of the quinoxaline ring binds to the backbone of His 283 (Fig. 2A). Because the water molecule in the hydrophobic pocket is no longer hydrogen bonded to the inhibitor, the water is pushed down further than that seen in co-crystal structures with a 2-pyridyl group in the hydrophobic pocket (Fig. 2B), although the hydrogen bonds between the water molecule and the protein residues (Glu 245, Tyr 249, and Asp 351) are maintained. The structural rearrangement that ensues does lead to a slightly larger hydrophobic pocket, which explains the tolerability of slightly larger groups in the *meta* position (Table 3) than has been seen in other vicinal biaryl TGFβ inhibitors.[6]

The selectivity of this class of inhibitors was tested by measuring the percent inhibition at 10 μM of compound **18** in a panel of 218 kinases at Upstate. Only two kinases, ALK4 at 76% and PKC alpha at 58% showed inhibition over 50%. These data suggest that members of this class of inhibitors can be highly selective TGFβR1 kinase inhibitors.

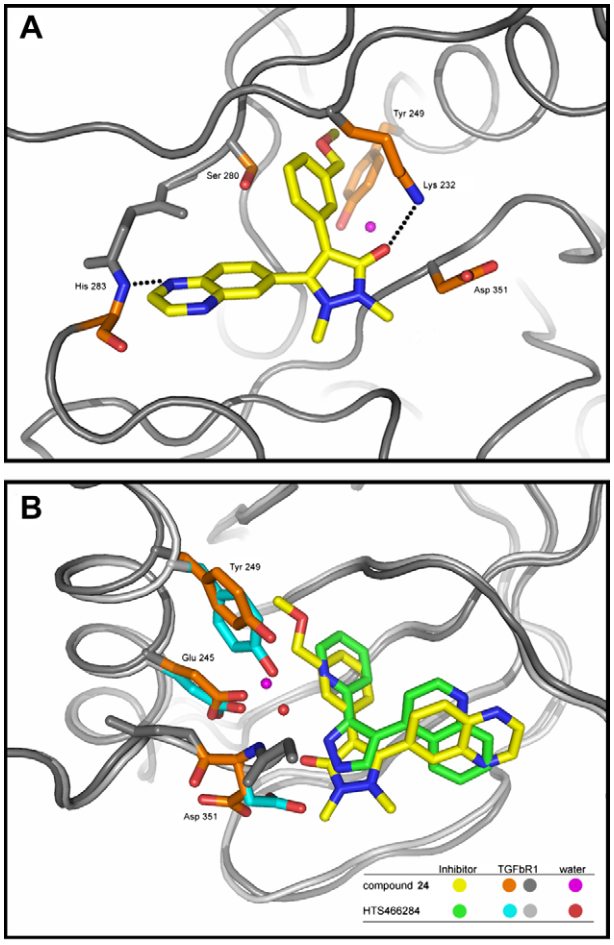

Figure 2. (A) Co-crystal structure of compound **24** and the kinase domain of TGFβR1 (PDB ID 3KCF). (B) Overlay of compound **24** with a published co-crystal structure of a vicinal biaryl pyrazole.[6]

The cellular potency of these analogs is also shown in Tables 1–4. The data show that at least a one order of magnitude loss in potency is seen when measuring TGFβR1 kinase inhibition inside the cell. The SAR seen in the cellular assay roughly tracks to that seen in the biochemical assay. We chose to take several of the compounds which showed cellular potency less than 500 nM and study them in vivo.

Oral bioavailability in general was poor in this series and suffered from high clearance. One exception, compound **33** showed 34% oral bioavailability at 5 mg/kg in rat with a 3 hour half life.[10] Compound **33** was further studied in a surrogate efficacy model developed to monitor TGFβR1 kinase inhibition using imaging. At 5 mg/kg in mice a 43% inhibition of TGFβ signaling was seen relative to vehicle control.[11]

The pyrazolone series described above has a novel pharmacophore pattern relative to currently published TGFβR1 kinase inhibitors that allows replacement of the ubiquitous nitrogen H-bond acceptor within the core with a carbonyl without significant loss in biochemical potency. Although the cellular potency and oral bioavailability in general were poor relative to other series, compound **33** showed significant TGFβR1 kinase inhibition in a surrogate efficacy model in mice.

Acknowledgment

We thank Dr. Cathy Sukow for assistance in generating Figure 2.

References and notes

1. Yingling, J. M.; Blanchard, K. L.; Sawyer, J. S. *Nat. Rev. Drug Disc.* **2004**, *3*, 1011.
2. Bierie, B.; Moses, H. L. *Nat. Rev. Cancer* **2006**, *6*, 506.
3. Kim, D. -K.; Jang, Y.; Lee, H. S.; Park, H. J.; Yoo, J. *J. Med. Chem.* **2007**, *50*, 3143.
4. Li, H. Y.; Wang, Y.; Heap, C. R.; King, C. H. R.; Mundla, S. R.; Voss, M.; Clawson, D. K.; Yan, L.; Campbell, R. M.; Anderson, B. D.; Wagner, J. R.; Britt, K.; Lu, K. X.; McMillen, W. T.; Yingling, J. M. *J. Med. Chem.* **2006**, *49*, 2138.
5. Sawyer, J. S.; Beight, D. W.; Britt, K. S.; Anderson, B. D.; Campbell, R. M.; Goodson, T.; Herron, D. K.; Li, H. Y.; McMillen, W. T.; Mort, N.; Parsons, S.; Smith, E. C. R.; Wagner, J. R.; Yan, L.; Zhang, F. M.; Yingling, J. M. *Bioorg. Med. Chem. Lett.* **2004**, *14*, 3581.
6. Singh, J.; Chuaqui, C. E.; Boriack-Sjodin, P. A.; Lee, W. C.; Pontz, T.; Corbley, M. J.; Cheung, H. K.; Arduini, R. M.; Mead, J. N.; Newman, M. N.; Papadatos, J. L.; Bowes, S.; Josiah, S.; Ling, L. E. *Bioorg. Med. Chem. Lett.* **2003**, *13*, 4355.
7. K_i values were determined using the Cheng–Prusoff equation from IC_{50}s for displacement of a labeled TGFβRI kinase inhibitor, HTS446284, 4-(3-pyridin-2-yl-1H-pyrazol-4-yl)-quinoline6, from purified recombinant TGFβRI kinase domain. Inhibition of cellular TGFβRI activity was determined by incubation of the test compound with HepG2 cells harboring a TGFβ signaling reporter, PAI-luciferase. These assays are described in detail in Ref. 9.
8. Sawyer, S. J.; Anderson, B. D.; Beight, D. W.; Campbell, R. M.; Jones, M. L.; Herron, D. K.; Lampe, J. W.; McCowan, J. R.; McMillan, W. T.; Mort, N.; Parsons, S.; Smith, E. C. R.; Vieth, M.; Wier, L. C.; Yan, L.; Zhang, F.; Yingling, J. M. *J. Med. Chem.* **2003**, *36*, 3953.
9. Fu, K.; Corbley, M. J.; Sun, L.; Friedman, J. E.; Shan, F.; Papadatos, J. L.; Costa, D.; Lutterodt, F.; Sweigard, H.; Bowes, S.; Boriack-Sjodin, P.-A.; Arduini, R. M.; Sun, D.; Newman, M. N.; Zhang, X.; Mead, J. N.; Chuaqui, C. E.; Cheung, H.-K.; Zhang, X.; Cornebise, M.; Carter, M.; Josiah, S.; Singh, J.; Lee, W.-C.; Gill, A.; Ling, L. E. *Arterio. Thromb. Vasc. Biol.* **2008**, *28*, 665.
10. PK parameters were determined by oral and iv administration of compound **33** at 5 mg/kg using 20% captisol as the vehicle. Eight time points were taken per arm and fitting of the curves and calculation of the PK parameters was performed with WinNonlin (Pharsight).
11. To evaluate the impact of ALK5 inhibitors on the TGFβ signaling pathway, Balb/C mice were injected with an adenoviral TGFβ inducible luciferase reporter intravenously. One day following adenoviral reporter administration, mice were first treated with a single oral dose of inhibitors or vehicle, and then challenged with 3 μg of recombinant human TGFβ protein injected into the peritoneal cavity 1 h later. The abilities of ALK5 inhibitors to block TGFβ inducible luciferase reporter expression in the animals were assessed at real-time non-invasively using the bioluminescence animal imaging IVISTM system according to manufacturer instructions (Caliper Life Sciences).